PASJ: Publ. Astron. Soc. Japan **46**, L97–L100 (1994)

An ASCA Observation of One Orbital Cycle of AR Lacertae

Nicholas E. WHITE,[1] Keith ARNAUD,[1,2] Charles S. R. DAY,[1,3] Ken EBISAWA,[1,3] Eric V. GOTTHELF,[1,3] Koji MUKAI,[1,3] Yang SOONG,[1,3] Tahir YAQOOB,[1,3] and Alex ANTUNES[4,5]

[1] *Laboratory for High Energy Astrophysics, Greenbelt, Maryland 20771, USA*
E-mail (NEW) white@heagip.gsfc.nasa.gov
[2] *University of Maryland*
[3] *University Space Research Association*
[4] *Institute of Space and Astronautical Science, 3-1-1 Yoshinodai, Sagamihara, Kanagawa 229*
[5] *Hughes STX*

(Received 1994 February 16; accepted 1994 March 23)

Abstract

An ASCA observation of one complete 2-day orbit of the eclipsing RS CVn binary AR Lac is reported. The time averaged X-ray spectrum reveals an emission line from Fe K at 6.7 keV, lines at lower energies from the Fe L complex, and K lines of Si, S, and other medium-Z elements. The previously established two-temperature thermal equilibrium emission model was fit to the spectra, but gives a poor fit. An improved fit is obtained if the abundance of O, Mg, Si, S, Ar, Ca, and Fe are 2–4 times less than the solar photospheric value. The underabundance of these elements lends support to the idea that weaker than expected absorption lines in the optical spectra of the secondary stars in RS CVn binaries are caused by these stars being metal poor. The overall orbital lightcurve is similar to that seen previously with a 50% reduction in flux centered on the primary eclipse and energy independent across the 0.4–7 keV band. At energies >2 keV the lightcurve shows continuous low level flaring activity on a timescale of 20–60 min.

Key words: Stars: abundances — Stars: binaries: eclipsing — Stars: individual (AR Lac)

1. Introduction

AR Lac is a 1.98-d eclipsing RS CVn binary containing a 2.81-$R_{\odot}$ K0 IV secondary and a 1.54-$R_{\odot}$ G2 IV primary. It is located at a distance of 50 pc and has an X-ray luminosity of $\sim 10^{31}$erg s^{-1}. AR Lac is one of the brightest stellar coronal X-ray sources in the sky. The X-ray spectrum shows two thermal components: one *hot* with a temperature of 20–40 million degrees and the second *cool* at 5–7 million degrees (Swank et al. 1981; Lemen et al. 1989). Both Einstein and EXOSAT imaging observations have shown that 50% of the 0.1–1.5 keV X-ray flux is eclipsed during primary eclipse and that the soft X-ray emission comes from discrete solar-like coronal structures on the G star (Walter et al. 1983; White et al. 1990). Above 2 keV the same EXOSAT observation showed the amplitude of the eclipse to be much reduced, suggesting the hotter component comes from large stellar sized regions (White et al. 1990). A recent ROSAT AR Lac observation by Ottmann, Schmitt, and Kurster (1993) show no evidence for a reduced eclipse amplitude above 1 keV. Spectroscopy by Ginga in the 2–10 keV band of the related RS CVn systems II Peg and UX Ari reveal a 6.7 keV Fe K line. The equivalent width of this line is a factor of 3–4 less than expected for emission from a solar abundance plasma in collisional equilibrium (Tsuru et al. 1989, Doyle et al. 1991).

In this letter we report the key results from an ASCA observation covering one orbital cycle of AR Lac. The extended 0.4–10.0 keV energy range of the ASCA imaging detectors, combined with superior energy resolution allows an improved study of the line emission, and the energy dependent properties of the X-ray eclipse.

2. Observations and Results

The ASCA observatory and its instrumentation are described in Tanaka et al. (1994). The observation of AR Lac began on 1993 June 1, 09:23 and ended June 3, 11:45 UT, and covered slightly over one orbital cycle. The instruments consist of two solid state imaging spectrometers (SIS) and two gas imaging spectrometers (GIS) with each detector at the focus of an imaging thin foil grazing incidence optics. Each SIS consists of four CCD chips, and for this observation were operated in 1-CCD mode, giving a time resolution of 4 s. Each GIS is a gas scintillation proportional counter. The full width half maximum energy resolution of each SIS is $\sim$ 60–120 eV

Table 1. Best fit parameters to the SIS 0 spectrum.

Parameter	*meka*	$\Delta\chi^2$	*RS*	$\Delta\chi^2$
EM_1 (cm^{-3})	3.0×10^{53}	...	3.5×10^{53}	...
kT_1 (keV)	0.58 ± 0.01	...	0.79 ± 0.01	...
EM_2 ($cm^{\mp 3}$)	4.9×10^{53}	...	4.9×10^{53}	...
kT_2 (keV)	1.96 ± 0.04	...	1.92 ± 0.04	...
N (1.12×10^{-4})	< 0.1	38	< 0.1	30
O (8.51×10^{-4})	0.38 ± 0.05	170	0.41 ± 0.06	87
Ne (1.23×10^{-4})	1.63 ± 0.15	45	1.33 ± 0.15	12
Mg (3.80×10^{-5})	0.67 ± 0.07	33	0.38 ± 0.06	103
Si (3.55×10^{-5})	0.44 ± 0.05	129	0.26 ± 0.04	172
S (1.62×10^{-5})	0.26 ± 0.06	132	0.20 ± 0.05	176
Ar (3.63×10^{-6})	0.34 ± 0.17	14	0.45 ± 0.15	13
Ca (2.29×10^{-6})	0.16 ± 0.25	12	0.34 ± 0.22	8
Fe (4.68×10^{-5})	0.32 ± 0.03	426	0.26 ± 0.03	220
Ni (1.78×10^{-6})	1.32 ± 0.25	1	0.72 ± 0.16	5

from 1–6 keV, compared to 200–600 eV for each GIS. The time resolution is 62.5 or 500 ms, depending on the telemetry bit rate. In 1-CCD mode the SIS cameras field of view is $11' \times 11'$. Each GIS has a $40'$ diameter circular field of view. AR Lac was detected with an average count rate of 1.2 ct s^{-1} in each SIS and 0.4 ct s^{-1} in each GIS.

A lightcurve was generated for each SIS by summing the counts over the whole CCD chip. Data were rejected when the telescope viewing direction was $< 25°$ from the bright earth limb (to exclude X-rays and light from the bright earth) and $< 10°$ from the dark earth. Hot and flickering pixels in the SIS were cleaned. For each GIS, a circular source region of radius $6'$ was used. GIS data with an earth elevation angle of $< 10°$ were rejected.

The observation started at binary phase 0.10 and ended at phase 1.16 (using the ephemeris JD 2444114.3431 + 1.9831674E; Kim 1991). Figure 1 shows the summed count rate recorded in the SIS detectors in the 0.4–1.1 keV band and in the GIS detectors between 2.0–7.0 keV band. The data have been folded on the orbital period (repeated for one half of an orbital cycle for clarity), and renormalized to the mean count rate. There is a 50% reduction in flux centered on the primary eclipse, with a gradual ingress starting at phase 0.85, well before first contact at phase 0.95. There is a shallow minimum around the time of secondary eclipse. A notable feature of the 2.0–7.0 keV lightcurve is that there are flares lasting 20–60 min. The overall orbital modulation shows no strong energy dependence, with the depth of the primary eclipse above 2 keV similar to that at lower energies.

In this letter we will concentrate on the spectral data obtained by one of the SIS instruments, SIS 0. A spectrum was accumulated for the entire observation within a circular region with a radius of $4'$ centered on the source. A background was taken from the outer regions of the CCD chip, where counts from the outer wings of the mirror point spread function are minimized. A total exposure time of 75000 s was obtained.

The SIS 0 X-ray spectrum is shown in figure 2. An Fe K emission line is detected at 6.7 keV, as well as structure at lower energies caused by emission lines from the Fe L complex, K lines from Si, S, and other medium-z elements. The Raymond and Smith (1978, *RS*) and the Mewe-Kaastra (Mewe, Gronenschild, van den Oord 1985; Kaastra 1992—*meka*) spectral models for emission from a plasma in thermal equilibrium were fit to the spectra. The fits are not strongly dependent on the interstellar absorption and its value was fixed at 1.0×10^{19} H cm^{-2} (cf. White et al. 1990). The results of a fit to a two temperature, 2T, *meka* model is shown in figure 2, assuming solar abundances. The fit is not acceptable with a reduced χ^2_ν of 4.39 (with 309 degrees of freedom). The χ^2 contribution of each spectral bin shows a large excess in the residuals around 0.7–3 keV, and that the Fe line around 6.7 keV is weaker than predicted. A solar abundance *RS* model also gives a poor fit, with a reduced χ^2_ν of 5.66. The residuals for both the *RS* and *meka* models show similar trends.

Allowing the abundance of the major line contributing elements to vary gives an improved fit with a χ^2_ν of 1.65 for a *RS* and 1.49 for a *meka*. The best fit to the data and the χ^2 residuals for the variable abundance *meka* model are shown in figure 2. While there is still some excess structure in the residuals around 1 keV, the overall fit is much improved. In table 1 we summarize the best fit parameters and one sigma uncertainties for both models. The assumed solar abundances are listed (Anders, Grevesse 1989) and the best fit values given relative to solar for each element. The best fit abundances are comparable in both the *meka* and *RS* models. The elements O, Mg, Si, S, Ar, Ca, and Fe are a factor of 2–4 below the solar value. The interdependance of the abundance measurements was determined by setting each element to solar values, and finding the $\Delta\chi^2$ after reminimizing χ^2. The $\Delta\chi^2$ values, given in table 1, show for both models that the fits are very sensitive to abundance variations of O, Si, S, and Fe. Also Mg is sensitive to abundance in the *RS* model, but not so much in *meka*, suggesting differences in the underlying plasma code. For Ar and Ca the abundances are not well determined, but still show the same downward trend. The fits require N to have an abundance < 0.1 solar, which seems extreme. Ni and Ne are consistent with solar abundance.

We obtained a ROSAT PSPC observation simultaneously with ASCA. The ROSAT data extend the energy range coverage down to 0.1 keV, albeit with a factor of 6–7 worse energy resolution at 1 keV than the SIS. A PSPC spectrum was accumulated for the entire observation (4900 s). A 2T solar abundance *RS* model gave

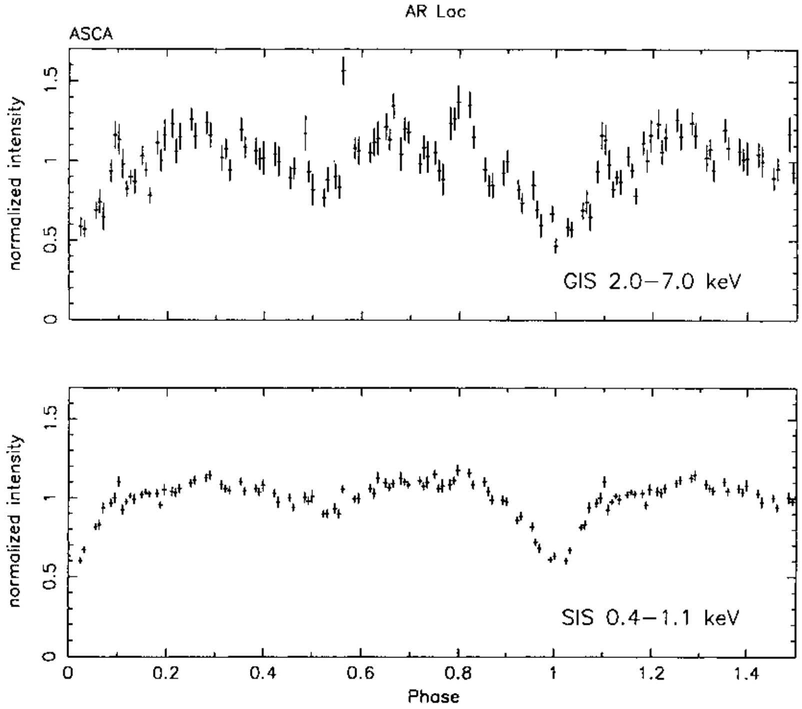

Fig. 1. The X-ray orbital lightcurve of AR Lac as measured by the ASCA SIS and GIS detectors in two energy bands. The 0.4–1.1 keV counting rate come from both SIS, and the 2.0–7.0 keV band from the two GIS. The data have been folded on the orbital period, and the lightcurve repeated for half a cycle for clarity. The accumulation time is 1338 s and the uncertainties are one sigma.

a poor fit with a χ^2_ν of 6.5 and low temperatures compared to ASCA of 0.2 and 1.0 keV. Varying the abundances globally gave an acceptable fit, with temperatures of 0.48 ± 0.14 keV and 1.2 ± 0.2 keV, an abundance of 0.29 ± 0.08 solar and a χ^2_ν of 1.18. The 2-keV high energy cutoff of the PSPC means that the best fit is not strongly dependent on the temperature of the hotter component and fixing it at the ASCA value of 2 keV only increases χ^2_ν to 1.66. This causes the temperature of the cooler component to increase to 0.73 keV and the abundance decrease to 0.20. These values are reasonably consistent with the ASCA values (table 1).

3. Discussion

The emission lines in the ASCA X-ray spectrum of AR Lac are weaker than expected. The simplest explanation is a factor of 3–4 underabundance of the medium-z elements in the AR Lac corona. The Fe underabundance is comparable to that found from other RS CVn systems by Ginga (Tsuru et al. 1989). The abundances determined using the *RS* and *meka* models (table 1) are comparable, within the uncertainties. Although the final fits are formally unacceptable, the residuals indicate this to be due to small problems around 1 keV, which may reflect uncertainties and approximations in the atomic physics. The solar corona shows enhanced abundance for elements with low first ionization potential, FIP, such as Si, Mg, and Ni (e.g., McKenzie, Feldman 1992). The under abundances found by ASCA are contrary to this trend. However, the optical absorption lines of the secondary stars in RS CVn systems like AR Lac are weaker than expected from model atmosphere calculations, and taken literally imply reduced abundances comparable to those required here (e.g., Naftilan, Drake 1977). Because it is unclear how two similar stars in a close binary system could have a factor of 5–10 difference in metallicity, the underabundance has been attributed to other causes, e.g., chromospheric activity somehow filling in the absorption lines. While ASCA can only determine the coronal abundance, it is notable that these values are comparable to the values found for the photosphere of the secondaries.

The temperatures and emission measures measured by ASCA for the two components are similar to those reported by White et al. (1990), Lemen et al. (1989), and Swank et al. (1981). But they are different from those reported by Ottmann et al. (1993) who using the ROSAT PSPC found systematically lower temperatures. The rel-

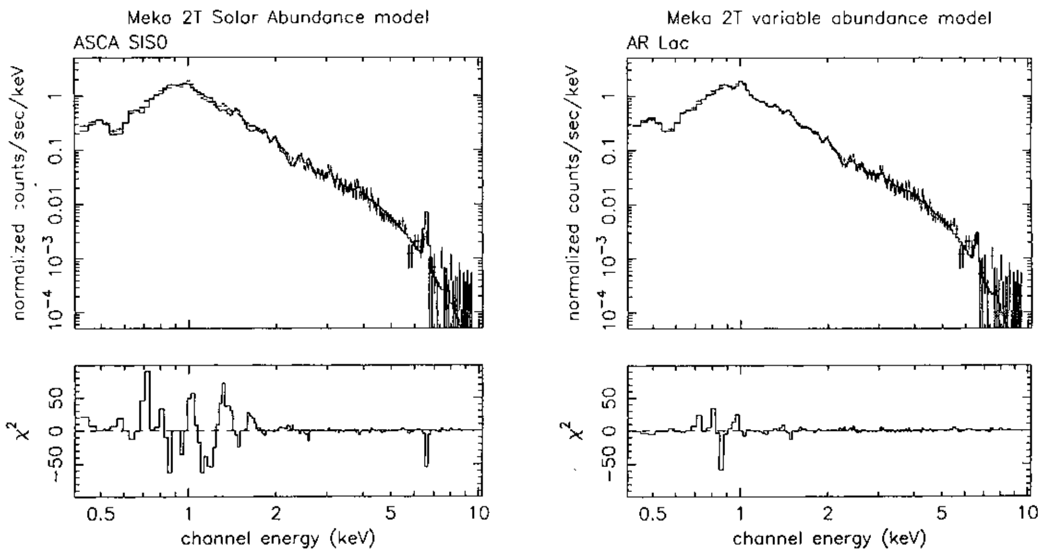

Fig. 2. The best fit to the SIS 0 spectra for a solar photospheric abundance two temperature *meka* model (left) and a variable abundance *meka* model (right). The residuals are given in the lower panels as the χ^2 contributions to each bin.

atively short accumulation times used by Ottmann et al. (1993) of 600–2000 s (driven by a requirement to have 6000 counts per spectrum) were insufficient to detect variances from solar abundance. Our ROSAT spectrum has 27000 counts and with these statistics the simple 2T model does not fit. Reducing the abundances to the ASCA values gives a good fit and increases the temperature of the two components to be in agreement with the ASCA values.

The ASCA 0.4–2 keV orbital lightcurve is similar to that observed previously in that energy band. The amplitude of the ASCA > 2 keV lightcurve is similar to that seen at lower energies, which is contrary to an earlier EXOSAT observation (White et al. 1990). This confirms and strengthens a ROSAT result where no energy dependance was found over the 0.1–2 keV band (Ottmann et al. 1993). A feature of the ASCA 2–7 keV lightcurve is continuous flare activity lasting 20–60 min. Part of the hot component may be associated with the flaring. The orbital modulation is superposed on this activity. During the EXOSAT observation a flare preceeded the primary eclipse, and this, plus other unresolved low-level flares may have filled in the X-ray eclipse.

We thank Steve Drake for useful discussions, the entire ASCA team and HEASARC staff for their support, and Jeff Linsky for a helpful referee report.

References

Anders E., Grevesse N. 1989, Geochim. Cosmochim. Acta 53, 197
Doyle J.G. et al. 1991, MNRAS 248, 503
Kaastra J.S. 1992, An X-Ray Spectral Code for Optically Thin Plasmas (SRON-Leiden Report)
Kim C.-H. 1991, AJ 102, 1784
Lemen J.R., Mewe R., Schrijver C.J., Fludra A. 1989, ApJ 341, 474
McKenzie D.L., Feldman U. 1992, ApJ 389, 764
Mewe R., Gronenschild E.H.B.M., and van den Oord G.H.J. 1985, A&AS 62, 197
Naftilan S.A., and Drake S.A. 1977, ApJ 216, 508
Ottmann R., Schmitt J.H.M.M., Kurster M. 1993, ApJ 413, 710
Raymond J.C., Smith B.W. 1977, ApJS 35, 419
Swank J.H. et al. 1981, ApJ 246, 208
Tanaka Y., Inoue H., Holt S.S. 1994, PASJ 46, L37
Tsuru, T. et al. 1989, PASJ 41, 679
Walter F., Gibson D.M., Basri G.S. 1983, ApJ 267, 665
White N.E. et al. 1990, ApJ 350, 776